Supplemental Material for
Amplified opto-mechanical transduction of virtual radiation pressure

Mauro Cirio,[1] Kamanasish Debnath,[1,2] Neill Lambert,[1] and Franco Nori[1,3]

[1] *CEMS, RIKEN, Wako-shi, Saitama 351-0198, Japan*
[2] *EPFL, CH-1015 Lausanne, Switzerland*
[3] *Department of Physics, University of Michigan, Ann Arbor, Michigan 48109-1040, USA*

In this supplemental material we present the details of the hybrid opto-mechanical structure considered in the main text. The system consists of an electromagnetic mode ultrastrongly coupled to a matter degree of freedom (via dipole interaction) and to a mechanical oscillator (via radiation pressure). In this way, the mechanical mode can be used as a probe of the dressed structure of the light-matter system, i.e., as a transducer of virtual radiation pressure. To amplify the signal, we consider a modulation of the opto-mechanical interaction at the mechanical frequency. We model the matter as either a spin (in the low-energy limit) or a bosonic mode and find a unified effective master equation (with different parameters) which describe them. We use these results to calculate bounds on the minimal amount of resources necessary to resolve virtual radiation-pressure effects when probing the mechanical quadratures. We finally present an analysis of experimental feasibility in an electro-mechanical setting.

I. LOW-ENERGY BOSONIZED LIGHT-MATTER-MECHANICAL MODEL

In this section, we derive the effective Hamiltonian to describe the low-energy physics of opto-mechanical systems where the cavity mode interacts ultrastrongly with a two-level atom (spin). In turn, such a model can be used to exactly describe the case where the matter degree of freedom can be directly modelled as bosonic. For symmetry, throughout this supplemental material the cavity mode has been relabelled as $a \mapsto a_1$.

A. Spin case

We consider the standard physical situation in which a spin (described by the operator $\sigma_\pm$) resonantly interacts with an electromagnetic mode confined in a cavity (described by the operator a) whose frequency ω is modulated by the position $x = x_{\mathrm{zp}}(b + b^\dagger)$ of the mechanical mode b of frequency ω_m. The Hamiltonian can be written as [1, 2]

$$H = \omega(x)a_1^\dagger a_1 + \frac{\omega}{2}\sigma_z + \Omega(a_1^\dagger + a_1)(\sigma_+ + \sigma_-) + \omega_m b^\dagger b \ . \tag{1}$$

As mentioned in the main text, third-order interaction terms can arise from the modulation of the field strength at the atom position as a consequence of the mechanical motion. However, such contributions can be made negligible by tuning the position of the atom inside the cavity while still being close to the point of maximum intensity of the electric field [3]. Now, by expanding to first order in x, we obtain

$$H = H_R + \omega_m b^\dagger b + g_0 a_1^\dagger a_1 (b + b^\dagger) \ , \tag{2}$$

with the vacuum opto-mechanical coupling

$$g_0 = x_{\mathrm{zp}} \frac{\partial \omega}{\partial x}_{|x=0} \ , \tag{3}$$

and where the light matter system is described by the quantum Rabi Hamiltonian

$$H_{\mathrm{R}} = \omega a_1^\dagger a_1 + \frac{\omega}{2}\sigma_z + \Omega(\sigma_+ + \sigma_-)(a_1 + a_1^\dagger) \ . \tag{4}$$

Here, we omitted zero-point energy contributions. We further considered the effect of this omission in section III. The ultrastrong coupling regime for the light-matter system (occurring when the normalized Rabi coupling

$$\eta = \frac{\Omega}{\omega} \geq 0.1 \ , \tag{5}$$

implies a perturbative characterization of the environment [4, 5] which induces transitions between Rabi dressed eigenstates. For this reason, we define a low-energy effective model by

$$H^{\text{eff}} = PHP \ , \tag{6}$$

where P is the projector into a low energy sector of the full Hilbert space

$$P = |G\rangle\langle G| + |-\rangle\langle -| + |+\rangle\langle +| \ , \tag{7}$$

where $|G\rangle\,, |\pm\rangle$ are the three energy eigenstates of the Rabi Hamiltonian H_R with lowest energy (not to be confused with the eigenstates of the Jaynes Cummings Hamiltonian denoted as $|0, g\rangle$ and $|n, \pm\rangle$). By using quasi-degenerate perturbation theory, at second order in η, these states are found to be

$$\begin{aligned} |G\rangle &= (1 - \tfrac{\eta^2}{8})\,|0, g\rangle + \tfrac{\eta}{2\sqrt{2}}(|2, -\rangle - |2, +\rangle) + \tfrac{\eta^2}{4}(|2, -\rangle + |2, +\rangle) \\ |\pm\rangle &= (1 - \tfrac{\eta^2}{8} - \tfrac{\eta^2}{32})\,|1, \pm\rangle \mp \tfrac{\eta}{4}(1 \pm \tfrac{\eta}{2})\,|1, \mp\rangle + (\tfrac{\eta}{2\sqrt{2}} \pm \tfrac{\eta^2}{8\sqrt{2}})(|3, -\rangle - |3, +\rangle) + \tfrac{\sqrt{3}\eta^2}{4\sqrt{2}}(|3, -\rangle + |3, +\rangle) \ , \end{aligned} \tag{8}$$

where

$$\begin{aligned} |0\rangle &= |0, g\rangle \\ |n, \pm\rangle &= \tfrac{|n,g\rangle \pm |n-1,e\rangle}{\sqrt{2}} \ , \end{aligned} \tag{9}$$

for $n \geq 1$ and where $|n, g/e\rangle$ are the eigenstates of $a^\dagger a$ and σ_z, i.e., they fulfill $a_1\,|0, g\rangle = \sigma^-\,|0, g\rangle = 0$, and $a_1^\dagger a_1\,|n, g\rangle = n\,|n, g\rangle$, $a_1^\dagger a_1\,|n, e\rangle = n\,|n, e\rangle$ and $\sigma_z\,|n, g\rangle = -\,|n, g\rangle$, $\sigma_z\,|n, e\rangle = |n, e\rangle$. At the same order, the corresponding energies are

$$\frac{\tilde{E}_0}{\omega} = -\frac{1}{2} - \frac{\eta^2}{2} + O(\eta^3) \ , \qquad \frac{\tilde{\omega}_\pm}{\omega} = \frac{1}{2} \pm \eta - \frac{\eta^2}{2} + O(\eta^3) \ . \tag{10}$$

Moreover, we have the following identities

$$\begin{aligned} \xi &\equiv \langle G|\, a_1^\dagger a_1\, |G\rangle = \tfrac{\eta^2}{4} \\ \tilde{\alpha}_\pm &\equiv \langle \pm|\, a_1^\dagger a_1\, |\pm\rangle = \tfrac{1}{2} \mp \tfrac{\eta}{4} + \tfrac{\eta^2}{4} \\ &\quad\ \langle \pm|\, a_1^\dagger a_1\, |\mp\rangle = \tfrac{1}{2} + \tfrac{3}{16}\eta^2 \\ &\quad\ \langle G|\, a_1^\dagger a_1\, |\pm\rangle = 0 \ . \end{aligned} \tag{11}$$

These results allow us to write

$$H^{\text{eff}} = H_R^{\text{eff}} + g_0(b + b^\dagger)(\tilde{\alpha}_-|-\rangle\langle -| + \tilde{\alpha}_+|+\rangle\langle +| + \xi|G\rangle\langle G|) + \omega_m b^\dagger b \ , \tag{12}$$

where

$$H_R^{\text{eff}} = \tilde{E}_0|G\rangle\langle G| + \tilde{\omega}_-|-\rangle\langle -| + \tilde{\omega}_+|+\rangle\langle +| \ , \tag{13}$$

and where we omitted terms proportional to the operators $|\pm\rangle\langle\mp|$ in a rotating-wave approximation. The omission of these terms requires careful analysis. In fact, in the interaction picture described by the diagonalized Rabi Hamiltonian, these operators rotate at frequencies $\pm 2\eta\omega$. However, the error produced by this approximation should not wash out the effect of the term $g_0\xi(b + b^\dagger)|G\rangle\langle G|$, which is the one giving rise to the physics we are exploring. For example, by using second order Van-Vleck perturbation theory in Floquet space [6–9], it is possible to show that, in a regime where $g_0/\eta\omega \ll 1$, the worst case errors are $O(g_0^2/\eta\omega)$ so that

$$\frac{g_0}{\omega} \ll \eta\xi \propto \eta^3 \ , \tag{14}$$

is enough to justify this approximation. Interestingly, this procedure critically requires the ultrastrong coupling regime.

As routinely done in condensed matter physics, within the low-energy approximation considered here, we now map our model to a purely bosonic one. In turn, this will allow us to extend our analysis to physical systems where a bosonic approximation for matter degrees of freedom can be done *a priori*, i.e., directly in the original Rabi Hamiltonian (see next subsection). With this idea in mind, we first re-write the previous Hamiltonian as

$$H^{\rm eff} = \omega_-|-\rangle\langle -| + \omega_+|+\rangle\langle +| + g_0(b+b^\dagger)(\alpha_-|-\rangle\langle -| + \alpha_+|+\rangle\langle +| + \xi) + \omega_m b^\dagger b \ , \tag{15}$$

where

$$\begin{array}{rclcl} \omega_\pm &=& \tilde{\omega}_\pm - \tilde{E}_0 &=& (1\pm\eta)\omega \\ \alpha_\pm &=& \tilde{\alpha}_\pm - \xi &=& (\frac{1}{2}\mp\frac{\eta}{4}) \ , \end{array} \tag{16}$$

and where we used the fact that, within the low-energy sector of the Hilbert space the relation

$$\mathbb{I} = |G\rangle\langle G| + |-\rangle\langle -| + |+\rangle\langle +| \ , \tag{17}$$

holds as an effective identity. Now, the bosonization of the previous Hamiltonian can be carried on by imposing the substitution $|G\rangle\langle\pm| \mapsto a_\pm$ to get

$$H^{\rm eff} = \omega_- a_-^\dagger a_- + \omega_+ a_+^\dagger a_+ + g_0(b+b^\dagger)(\alpha_- a_-^\dagger a_- + \alpha_+ a_+^\dagger a_+ + \xi) + \omega_m b^\dagger b \ . \tag{18}$$

By considering a modulation $g_0 \mapsto g_0\cos\omega_m t$, by going to a frame rotating at the mechanical frequency [10–13], and by subsequently performing a rotating wave approximation, we then exactly get Eq. (10) as reported in the main text.

B. Bosonic matter

In a physical situation where the matter degree of freedom can be modelled as bosonic *a priori*, we can directly start our analysis by imposing the substitutions $\sigma_- \mapsto a_2$ in Eq. (2), i.e., by replacing the spin with a harmonic oscillator with annihilation operator a_2. Explicitly

$$H^B = \omega a_1^\dagger a_1 + \omega a_2^\dagger a_2 + \Omega(a_1+a_1^\dagger)(a_2+a_2^\dagger) + \omega_m b^\dagger b + g_0 a_1^\dagger a_1 (b+b^\dagger) \ . \tag{19}$$

For $g_0=0$, this model is solvable and, by defining $a_\pm = (m\omega_\pm/2)^{1/2}[x_\pm + i/(m\omega_\pm)p_\pm]$, in terms of $x_\pm = x_1 \pm x_2/\sqrt{2}$, where $x_j = (2m\omega)^{-1/2}(a_j + a_j^\dagger)$ (j=1,2), we obtain, after some straightforward algebra

$$\begin{aligned} H^B \;=\; & E_0 + \omega_+^B a_+^\dagger a_+ + \omega_-^B a_-^\dagger a_- + \omega_m b^\dagger b + g_0(b+b^\dagger)\{\frac{1}{8\omega\omega_+^B}[(\omega^2-\omega_+^{B\,2})(a_+^\dagger a_+^\dagger + a_+a_+)] + \frac{1}{4\omega\omega_+^B}[(\omega^2+\omega_+^{B\,2})a_+^\dagger a_+] \\ & + \frac{1}{8\omega\omega_-^B}[(\omega^2-\omega_-^{B\,2})(a_-^\dagger a_-^\dagger + a_-a_-)] + \frac{1}{4\omega\omega_-^B}[(\omega^2+\omega_-^{B\,2})a_-^\dagger a_-]\} + g_0(b+b^\dagger)[\frac{(\omega-\omega_+^B)^2}{8\omega\omega_+^B} + \frac{(\omega-\omega_-^B)^2}{8\omega\omega_-^B}] \\ & + g_0(b+b^\dagger)\left\{\frac{1}{4\omega\sqrt{\omega_+^B\omega_-^B}}(\omega^2-\omega_+^B\omega_-^B)(a_+^\dagger a_-^\dagger + a_+a_-) + \frac{1}{4\omega\sqrt{\omega_+^B\omega_-^B}}(\omega^2+\omega_+^B\omega_-^B)(a_+^\dagger a_- + a_-^\dagger a_+)\right\} \ , \end{aligned} \tag{20}$$

where $E_0 = (\omega_+^B+\omega_-^B)/2-\omega$, $\omega_\pm^B = \omega(1\pm 2\eta)^{1/2}$, and where, explicitly, the Bogoliubov relations reads

$$a_j + a_j^\dagger = \sqrt{\frac{\omega}{2\omega_+^B}}(a_+ + a_+^\dagger) + (-1)^j\sqrt{\frac{\omega}{2\omega_-^B}}(a_- + a_-^\dagger) \ , \tag{21}$$

for $j=1,2$. We now notice that terms proportional to $a_\pm^\dagger a_\pm^\dagger$ and $a_\pm a_\pm$ rotate at frequencies $\pm 2\omega_\pm^B$ and can be neglected with a rotating-wave approximation. A similar analysis holds for the terms $a_+^\dagger a_-^\dagger$ and a_+a_-, at lowest order in η. The terms proportional to $a_+^\dagger a_-$ and $a_-^\dagger a_+$ rotate at a lower frequency (i.e., $O(\omega\eta)$) and their norm is suppressed by the factor η^2. For this reason, in order to neglect them, we need to carry the same perturbative considerations done in the spin case. In this approximation, we get our final result of this subsection

$$H^B \;=\; \omega_+^B a_+^\dagger a_+ + \omega_-^B a_-^\dagger a_- + \omega_m b^\dagger b + g_0(b+b^\dagger)(\alpha_+^B a_+^\dagger a_+ + \alpha_-^B a_-^\dagger a_- + \xi^B) \ , \tag{22}$$

with

$$\begin{aligned} \alpha_\pm^B \;&=\; \frac{(\omega^2+\omega_\pm^{B\,2})}{4\omega\omega_\pm^B} = \frac{(1+\eta)}{2\sqrt{1\pm 2\eta}} \simeq \tfrac{1}{2}+\tfrac{1}{4}\eta^2 \\ \xi^B \;&=\; \frac{(\omega-\omega_+)^2}{8\omega\omega_+} + \frac{(\omega-\omega_-)^2}{8\omega\omega_-} \simeq \tfrac{1}{4}\eta^2 = \xi \ , \end{aligned} \tag{23}$$

where the $\simeq$ equalities are valid at second order in η. It is interesting to note that the case $\eta = 0$ (i.e., the case in the absence of light-matter interaction) cannot be immediately recovered from Eq. (22). In fact, in this case, from Eq. (19), we should have

$$H(\eta = 0) = \omega a_1^\dagger a_1 + \omega a_2^\dagger a_2 + \omega_m b^\dagger b + g_0 a_1^\dagger a_1 (b + b^\dagger) \ , \tag{24}$$

which does not correspond to what can be found when substituting $\eta = 0$ in Eq. (22). This is simply due to the fact that in Eq. (22) we neglected terms rotating at frequencies proportional to $\omega\eta$, which is justified only in the ultrastrong coupling regime.

At zero temperature, while the radiation pressure in the absence of the atom is null $P_{\mathrm{GS}}^{\eta=0}$, in the presence of matter it takes a nonzero value, i.e., $P_{\mathrm{GS}}^{\eta} = g_0 \xi / x_{zp}$ in the spin case ($g_0 \xi^B / x_{zp}$ in the bosonic case). We note that, for high temperatures, the ratio between the two pressure still depends on η. While the low-energy analysis for the spin case prevent us from studying this high-temperature limit, in the bosonic case we immediately obtain

$$\frac{P^\eta}{P^{\eta=0}} = 1 + \frac{\eta^2}{2} \ , \tag{25}$$

in the case $n_+ = n_- = n$, and taking n to be the occupation number for the electromagnetic environment also in the absence of matter.

II. INTERACTION WITH ENVIRONMENT

In this section we show how to model the interaction with the environment for both bosonic and spin matter cases. To lighten the notation throughout the section we omit the suffix B for the parameters in the bosonic case.

A. Master equation for Bosonic Matter

To correctly describe the steady-state behavior of this system we must correctly describe its interaction with three independent baths, one for each subsystem,

$$H_{\mathrm{bath}} \ = \ H_{\mathrm{bath}}^0 + H_{\mathrm{bath}}^I \ , \tag{26}$$

where

$$\begin{aligned} H_{\mathrm{bath}}^0 \ &= \ \textstyle\sum_{\omega_j} \omega_j \left[t_1(\omega_j)^\dagger t_1(\omega_j) + t_2(\omega_j)^\dagger t_2(\omega_j) + t_b(\omega_j)^\dagger t_b(\omega_j) \right] \\ H_{\mathrm{bath}}^I \ &= \ \textstyle\sum_{\omega_j} \left[\lambda_1(\omega_j)(a_1 + a_1^\dagger)(t_1(\omega_j) + t_1^\dagger(\omega_j)) + \lambda_2(\omega_j)(a_2 + a_2^\dagger)(t_2(\omega_j) + t_2^\dagger(\omega_j)) + \lambda_m(\omega_j)(b + b^\dagger)(t_m + t_m^\dagger) \right] \ , \end{aligned} \tag{27}$$

in terms of bosonic annihilation operators t_1, t_2, t_m representing the baths interacting with the cavity, matter and mechanics respectively with interaction rates λ_1, λ_2, λ_m. By using the results of the previous section, we can substitute the Bogoliubov relations in Eq. (21) into H_{bath}^I to get

$$\begin{aligned} H_{\mathrm{bath}}^I \ = \ \sum_{\omega_j} \Bigg\{ & \sqrt{\frac{\omega}{2\omega_+}} (a_+ + a_+^\dagger) \left[\lambda_1(\omega_j) B_1(\omega_j) + \lambda_2(\omega_j) B_2(\omega_j) \right] + \sqrt{\frac{\omega}{2\omega_-}} (a_- + a_-^\dagger) \left[\lambda_1(\omega_j) B_1(\omega_j) - \lambda_2(\omega_j) B_2(\omega_j) \right] \\ & + \lambda_m(\omega_j)(b + b^\dagger)(t_m(\omega_j) + t_m^\dagger(\omega_j)) \big] \Bigg\} \ , \end{aligned} \tag{28}$$

where $B_1(\omega) = t_1(\omega) + t_1^\dagger(\omega)$ and $B_2(\omega) = t_2(\omega) + t_2^\dagger(\omega)$. Now, by defining

$$p_\pm(\omega_j) = \frac{\lambda_1(\omega_j) t_1(\omega_j) \pm \lambda_2(\omega_j) t_2(\omega_j)}{\sqrt{\lambda_1^2(\omega_j) + \lambda_2^2(\omega_j)}} \ , \tag{29}$$

we obtain (omitting ω_j dependences)

$$H_{\mathrm{bath}}^I \ = \ \textstyle\sum_{\omega_j} \lambda_+ (a_+ + a_+^\dagger)(p_+^\dagger + p_+) + \sum_{\omega_j} \lambda_- (a_- + a_-^\dagger)(p_-^\dagger + p_-) + \sum_{\omega_j} \lambda_m (b + b^\dagger)(t_m + t_m^\dagger) \big] \ , \tag{30}$$

where

$$\lambda_\pm = \left[\left(\frac{\omega}{\omega_j}\right)\frac{\lambda_1^2(\omega_j)+\lambda_2^2(\omega_j)}{2}\right]^{1/2} \quad , \tag{31}$$

and similarly for the free term

$$H^0_{\rm bath} = \sum_{\omega_j}\omega_j\left[p_+(\omega_j)^\dagger p_+(\omega_j) + p_-(\omega_j)^\dagger p_-(\omega_j) + t_m(\omega_j)^\dagger t_m(\omega_j)\right] \quad . \tag{32}$$

This shows the normal modes interact with independent baths. In this way we can immediately integrate out the baths to obtain a master equation which can be written as [14]

$$\dot\rho = -i[H,\rho] + \mathcal{L}_+(\rho) + \mathcal{L}_-(\rho) + \mathcal{L}_m(\rho) \ \ , \tag{33}$$

where

$$\begin{aligned} \mathcal{L}_\pm(\rho) &= \left[2\pi\textstyle\sum_{\omega_j}\lambda_\pm^2(\omega_j)\langle p_\pm^\dagger p_\pm\rangle\delta(\omega_j-\omega_\pm)\right]\mathcal{D}[a_\pm^\dagger](\rho) + \left[2\pi\textstyle\sum_{\omega_j}\lambda_\pm^2(\omega_j)(1+\langle p_\pm^\dagger p_\pm\rangle)\delta(\omega_j-\omega_\pm)\right]\mathcal{D}[a_\pm](\rho) \\ \mathcal{L}_m(\rho) &= \Gamma_m\left(n(T_m)\mathcal{D}[b^\dagger](\rho) + (1+n(T_m))\mathcal{D}[b](\rho)\right) \quad , \end{aligned} \tag{34}$$

where

$$\begin{aligned} \mathcal{D}[O](\rho) &= \tfrac{1}{2}(2O\rho O^\dagger - \rho O^\dagger O - O^\dagger O\rho) \\ \Gamma_m &= 2\pi d_m\lambda_m^2 \ \ , \end{aligned} \tag{35}$$

where d_m is the density of states for the mechanical bath associated with temperature T_m. By introducing the densities of states d_1, d_2 for the remaining modes, we can further simplify this result by explicitly computing

$$\begin{aligned} \textstyle\sum_{\omega_j}\lambda_\pm^2(\omega_j)(1+\langle p_\pm^\dagger p_\pm\rangle)\delta(\omega_j-\omega_\pm) &= \textstyle\sum_{\omega_j}\frac{\omega}{\omega_\pm}\frac{\lambda_1^2+\lambda_2^2}{2}\left(1+\frac{\lambda_1^2 n(\omega_j,T_1)+\lambda_2^2 n(\omega_j,T_2)}{\lambda_1^2+\lambda_2^2}\right)\delta(\omega_j-\omega_\pm) \\ &= \frac{\omega}{2\omega_\pm}\int d\bar\omega\ \delta(\bar\omega-\omega_\pm)\left[\lambda_1^2(\bar\omega)d_1(\bar\omega)(1+\bar n(\bar\omega,T_1)) + \lambda_2^2(\bar\omega)d_2(\bar\omega)(1+\bar n(\bar\omega,T_1))\right] \\ &= \frac{\omega}{2\omega_\pm}\left[\lambda_1^2(\omega_\pm)d_1(\omega_\pm)(1+\bar n(\omega_\pm,T_1)) + \lambda_2^2(\omega_\pm)d_2(\omega_\pm)(1+\bar n(\omega_\pm,T_1))\right] \\ \textstyle\sum_{\omega_j}\lambda_\pm^2(\omega_j)\langle p_\pm^\dagger p_\pm\rangle\delta(\omega_j-\omega_\pm) &= \frac{\omega}{2\omega_\pm}\left[\lambda_1^2(\omega_\pm)d_1(\omega_\pm)\bar n(\omega_\pm,T_1) + \lambda_2^2(\omega_\pm)d_2(\omega_\pm)\bar n(\omega_\pm,T_1)\right] \quad . \end{aligned} \tag{36}$$

We now define

$$\begin{aligned} \kappa_\pm &= 2\pi\frac{\omega}{2\omega_\pm}\left[d_1(\omega_\pm)\lambda_1^2(\omega_\pm) + d_2(\omega_\pm)\lambda_2^2(\omega_\pm)\right] \\ \kappa_\pm n_\pm &= 2\pi\frac{\omega}{2\omega_+}\left[d_1(\omega_\pm)\lambda_1^2(\omega_\pm)\bar n(\omega_\pm,T_1) + d_2(\omega_\pm)\lambda_2^2(\omega_\pm)\bar n(\omega_\pm,T_2)\right] \quad , \end{aligned} \tag{37}$$

where $\bar n_\pm = \bar n(\omega_\pm, T_\pm)$ and where we introduced the effective temperatures $T_\pm$ which can be found by solving the implicit equation

$$\bar n_\pm = \frac{d_1(\omega_\pm)\lambda_1^2(\omega_\pm)\bar n(\omega_\pm,T_1) + d_2(\omega_\pm)\lambda_2^2(\omega_\pm)\bar n(\omega_\pm,T_2)}{d_1(\omega_\pm)\lambda_1^2(\omega_\pm) + d_2(\omega_\pm)\lambda_2^2(\omega_\pm)} \quad , \tag{38}$$

as

$$k_{\rm B}T_\pm = \hbar\omega_\pm\left[\log\left(1+\frac{1}{\bar n(\omega_\pm,T_1)+\bar n(\omega_\pm,T_2)}\right)\right]^{-1} \quad . \tag{39}$$

As an immediate check, if we assume $T_1 = T_2 = T$ we get $\bar n_\pm = \bar n(\omega_\pm, T)$. In this way we can write the following simplified form for the Liouvillians

$$\mathcal{L}_\pm(\rho) \ = \ \kappa_\pm\left(\bar n_\pm\mathcal{D}[a_\pm^\dagger](\rho) + (1+\bar n_\pm)\mathcal{D}[a_\pm](\rho)\right) \quad , \tag{40}$$

where

$$\kappa_{\pm} = \frac{\omega}{\omega_{\pm}} \frac{\kappa_1 + \kappa_2}{2} \quad , \tag{41}$$

with

$$\begin{aligned} \kappa_1 &= 2\pi d_1(\omega_{\pm}) \lambda_1^2(\omega_{\pm}) \\ \kappa_2 &= 2\pi d_2(\omega_{\pm}) \lambda_2^2(\omega_{\pm}) \quad , \end{aligned} \tag{42}$$

are the rates if the systems were independently coupled to their baths (but evaluated at the polaritonic frequencies).
This result is general and has no temperature restrictions in this bosonic matter case. Below, we derive a master equation which can be used to model both the spin and bosonic matter cases in the low energy limit. When applied to the bosonic case, the result will match the one given in this section, as it logically should.

B. Master equation at low temperatures (for both boson and spin cases)

As mentioned above, in the ultrastrong coupling regime, the environment induces transitions between the dressed eigenstates. The master equation for the system can be written as [5]

$$\dot{\rho} = -i[H, \rho] + \mathcal{L}_1(\rho) + \mathcal{L}_2(\rho) + \mathcal{L}_m(\rho) \quad , \tag{43}$$

where

$$\begin{aligned} \mathcal{L}_1(\rho) &= \textstyle\sum_{j,k>j} \Gamma_1^{jk} \bar{n}(\Delta_{kj}, T_1) \mathcal{D}[|k\rangle \langle j|](\rho) + \sum_{j,k>j} \Gamma_1^{jk} (1 + \bar{n}(\Delta_{kj}, T_1)) \mathcal{D}[|j\rangle \langle k|](\rho) \\ \mathcal{L}_2(\rho) &= \textstyle\sum_{j,k>j} \Gamma_2^{jk} \bar{n}(\Delta_{kj}, T_2) \mathcal{D}[|k\rangle \langle j|](\rho) + \sum_{j,k>j} \Gamma_2^{jk} (1 + \bar{n}(\Delta_{kj}, T_2)) \mathcal{D}[|j\rangle \langle k|](\rho) \\ \mathcal{L}_m(\rho) &= \kappa \left(n(T_m) \mathcal{D}[b^\dagger](\rho) + (1 + n(T_m)) \mathcal{D}[b](\rho) \right) \quad , \end{aligned} \tag{44}$$

where $H = H^{\text{eff}}, H^B$, and where the indexes j, k label eigenstates of the system in increasing energy order and where

$$\begin{aligned} \Gamma_1^{jk} &= 2\pi d_1(\Delta_{kj}) \lambda_1^2(\Delta_{jk}) |\langle k| (a_1 + a_1^\dagger) |j\rangle|^2 \\ \Gamma_2^{jk} &= 2\pi d_2(\Delta_{kj}) \lambda_2^2(\Delta_{jk}) |\langle k| (a_2 + a_2^\dagger) |j\rangle|^2 \quad , \end{aligned} \tag{45}$$

in terms of the density of states of the bath d_1 and d_2 in the bosonic case and

$$\begin{aligned} \Gamma_1^{jk} &= 2\pi d_1(\Delta_{kj}) \lambda_1^2(\Delta_{jk}) |\langle k| (a_1 + a_1^\dagger) |j\rangle|^2 \\ \Gamma_2^{jk} &= 2\pi d_2(\Delta_{kj}) \lambda_2^2(\Delta_{jk}) |\langle k| (\sigma_- + \sigma_+) |j\rangle|^2 \quad , \end{aligned} \tag{46}$$

in the spin case (in this section the cavity mode will be denoted with a_1). We explicitly note that, as explained in [5], the degeneracies present in the bosonic case should pose a problem in the derivation of Eq. (43). However, in this case, the degeneracies are lifted at an effective level, by imposing the low energy approximation. This energy restriction amounts to considering as the only relevant states for the fields a_1 and a_2 the ground and first excited states. We can then write, for example

$$\begin{aligned} \textstyle\sum_{j,k>j} \Gamma_1^{jk} \bar{n}(\Delta_{kj}, T_1) \mathcal{D}[|k\rangle \langle j|](\rho) \simeq\ & 2\pi d_1(\omega_+) \lambda_1^2(\omega_+) |\langle +| (a_1 + a_1^\dagger) |G\rangle|^2 \bar{n}(\omega_+, T_1) \mathcal{D}[|+\rangle \langle G|](\rho) \\ & + 2\pi d_1(\omega_-) \lambda_1^2(\omega_-) |\langle -| (a_1 + a_1^\dagger) |G\rangle|^2 \bar{n}(\omega_-, T_1) \mathcal{D}[|-\rangle \langle G|](\rho) \quad . \end{aligned} \tag{47}$$

This is the point where differences due to the the spin or bosonic nature of the matter degree of freedom enter the analysis. This is simply due to different expressions for the transition matrix elements.
It is important to remark the reason for the absence of terms proportional to the operator $\mathcal{D}[\langle\pm| |\mp\rangle]$ in the master equation. In the spin case, we can first observe that the excited states $|\pm\rangle$ in Eq. (8) have an odd number of excitations. Since both $a_1 + a_1^\dagger$ and $\sigma_- + \sigma_+$ change the number of excitations by 1, all the matrix elements $\langle\pm| a_1 + a_1^\dagger |\mp\rangle$ and $\langle\pm| \sigma_+ \sigma_+ |\mp\rangle$ will be zero. In the bosonic case we can invoke the same reasoning which follows from the linear expression in Eq. (21).

1. Bosonic case

In the bosonic case, we can use the Bogoliubov transformations in Eq. (21) and evaluate the previous expression as

$$\sum_{j,k>j}\Gamma_1^{jk}\bar{n}(\Delta_{kj},T_1)\mathcal{D}[|k\rangle\langle j|](\rho) \simeq 2\pi[\rho_1(\omega_+)\lambda_1^2(\omega_+)\frac{\omega}{2\omega_+}\bar{n}(\omega_+,T_1)\mathcal{D}[a_+^\dagger](\rho)+\rho_1(\omega_-)\lambda_1^2(\omega_-)\frac{\omega}{2\omega_-}\bar{n}(\omega_-,T_1)\mathcal{D}[a_-^\dagger](\rho)] \ , \tag{48}$$

and analogously for the remaing terms in Eq. (43) to get

$$\dot{\rho} = -i[H,\rho]+\mathcal{L}_+(\rho)+\mathcal{L}_-(\rho)+\mathcal{L}_m(\rho) \ , \tag{49}$$

where

$$\begin{aligned}\mathcal{L}_\pm(\rho) \ &= \ 2\pi\frac{\omega}{2\omega_\pm}\left[d_1(\omega_+)\lambda_1^2(\omega_\pm)\bar{n}(\omega_\pm,T_1)+d_2(\omega_\pm)\lambda_2^2(\omega_\pm)\bar{n}(\omega_\pm,T_2)\right]\mathcal{D}[a_\pm^\dagger](\rho)\\ &+2\pi\frac{\omega}{2\omega_\pm}\left[d_1(\omega_\pm)\lambda_1^2(\omega_\pm)(1+\bar{n}(\omega_\pm,T_1))+d_2(\omega_\pm)\lambda_2^2(\omega_\pm)(1+\bar{n}(\omega_\pm,T_2))\right]\mathcal{D}[a_\pm](\rho) \ ,\end{aligned} \tag{50}$$

which, as promised, is in fact equivalent to the expression given in Eq. (34) (by immediate use of Eq. (36)), and all the subsequent analysis can be taken from there.

2. Spin case

In the spin case, the matrix coefficients take a different form which can be computed at second order in η by Eq. (8), and explicitly read

$$\begin{aligned}\zeta_a^\pm \equiv |\langle\pm|(a+a^\dagger)|G\rangle|^2 \ &= \ \tfrac{1}{2}|(1\mp\tfrac{3\eta}{4}+\tfrac{15\eta^2}{32})|^2 \ = \ \tfrac{1}{2}(1\mp\tfrac{\eta}{4}+\tfrac{\eta^2}{32})\\ \zeta_\sigma^\pm \equiv |\langle\pm|(\sigma_-+\sigma_+)|G\rangle|^2 \ &= \ \tfrac{1}{2}|(1\mp\tfrac{\eta}{4}+\tfrac{\eta^2}{32})|^2 \ = \ \tfrac{1}{2}(1\mp\tfrac{\eta}{2}+\tfrac{\eta^2}{8}) \ .\end{aligned} \tag{51}$$

Consequently, Eq. (47) in this case becomes

$$\begin{aligned}\sum_{j,k>j}\Gamma_1^{jk}\bar{n}(\Delta_{kj},T_1)\mathcal{D}[|k\rangle\langle j|](\rho) \ &\simeq \ 2\pi[\rho_1(\omega_+)\lambda_1^2\zeta_a^+\bar{n}(\omega_+,T_1)\mathcal{D}[a_+^\dagger](\rho)+\rho_1(\omega_-)\lambda_1^2(\omega_-)\zeta_a^-\bar{n}(\omega_-,T_1)\mathcal{D}[a_-^\dagger](\rho)]\\ \sum_{j,k>j}\Gamma_2^{jk}\bar{n}(\Delta_{kj},T_2)\mathcal{D}[|k\rangle\langle j|](\rho) \ &\simeq \ 2\pi[\rho_2(\omega_+)\lambda_2^2\zeta_\sigma^+\bar{n}(\omega_+,T_2)\mathcal{D}[a_+^\dagger](\rho)+\rho_2(\omega_-)\lambda_2^2(\omega_-)\zeta_\sigma^-\bar{n}(\omega_-,T_2)\mathcal{D}[a_-^\dagger](\rho)] \ ,\end{aligned} \tag{52}$$

leading to formally the same solution as in the bosonic case but with different rates

$$\begin{aligned}\kappa_\pm \ &= \ 2\pi\left[d_1(\omega_\pm)\zeta_a^\pm\lambda_1^2(\omega_\pm)+d_2(\omega_\pm)\zeta_\sigma^\pm\lambda_2^2(\omega_\pm)\right]\\ \kappa_\pm n_\pm \ &= \ 2\pi\left[d_1(\omega_\pm)\zeta_a^\pm\lambda_1^2(\omega_\pm)\bar{n}(\omega_\pm,T_1)+d_2(\omega_\pm)\zeta_\sigma^\pm\lambda_2^2(\omega_\pm)\bar{n}(\omega_\pm,T_2)\right] \ .\end{aligned} \tag{53}$$

In the case $T_1=T_2=T$ we get $\bar{n}_\pm=\bar{n}(\omega_\pm,T)$ as in the previous case and we can write the following simplified form for the Liouvillians

$$\mathcal{L}_\pm(\rho) \ = \ \kappa_\pm\left(\bar{n}_\pm\mathcal{D}[a_\pm^\dagger](\rho)+(1+\bar{n}_\pm)\mathcal{D}[a_\pm](\rho)\right) \ , \tag{54}$$

where $\kappa_\pm=\zeta_a^\pm\kappa_1+\zeta_\sigma^\pm\kappa_2$ with $\kappa_1=2\pi d_1(\omega_\pm)\lambda_1^2(\omega_\pm)$ and $\kappa_2=2\pi d_1(\omega_\pm)\lambda_1^2(\omega_\pm)$ are the rates if the systems were independently coupled to their baths (but evaluated at the polaritonic frequencies).

III. HEISENBERG EQUATION OF MOTION

In this section we first derive an expression for the quadrature averages and variances for the spin and bosonic cases. The different physical nature of these two models enters the derivation through a different expression for the parameters, as summarized in the following table.

	$\omega_\pm$	$\alpha_\pm$	ξ	$\kappa_\pm$
Spin Case	$(1\pm\eta)\omega$	$\frac{1}{2}\mp\frac{\eta}{4}$	$\frac{\eta^2}{4}$	$\zeta_a^\pm\kappa_1+\zeta_\sigma^\pm\kappa_2$
Bosonic Case	$\omega(1\pm 2\eta)^{1/2}$	$\frac{(\omega^2+\omega_\pm{}^2)}{4\omega\omega_\pm}\simeq\frac{1}{2}+\frac{1}{4}\eta^2$	$\frac{(\omega-\omega_+)^2}{8\omega\omega_+}+\frac{(\omega-\omega_-)^2}{8\omega\omega_-}\simeq\frac{\eta^2}{4}$	$\frac{\omega}{\omega_\pm}\frac{\kappa_1+\kappa_2}{2}$

For the spin case, the validity of the model is restricted to a low energy limit and at second order in η, which we require to be $\eta\simeq 0.1$ (ultrastrong coupling regime) to derive the master equation. The bosonic model is, in principle, exact at all temperatures. However, we notice that the rotating-wave approximation applied to obtain Eq. (22) also requires the condition $\eta^3\gg g_0/\omega$ to be satisfied.

Finally, in the last subsection, we then use the expressions for the quadratures to quantify the visibility of the effect considered in this article, i.e., the regime where virtual radiation pressure is observable for both bosonic and spin cases.

A. Solution

Let us now consider the Hamiltonian in Eq. (22)

$$H=\omega_+a_+^\dagger a_+ +\omega_-a_-^\dagger a_- +\omega_m b^\dagger b+\sqrt{2}g_0X\hat{\alpha}\ \ , \tag{55}$$

where the dimensionless quadratures are defined as $X=(b+b^\dagger)/\sqrt{2}$ and $\tilde{X}=i(b^\dagger-b)/\sqrt{2}$, and where $\hat{\alpha}=\alpha_+a_+^\dagger a_+ + \alpha_-a_-^\dagger a_- +\xi$.

The state of the system is described by a density matrix which satisfies

$$\dot{\rho}=-i[H,\rho]+\mathcal{L}_+(\rho)+\mathcal{L}_-(\rho)+\mathcal{L}_m(\rho)\ \ , \tag{56}$$

where $\mathcal{L}_\pm(\rho)=\kappa_\pm\left(\bar{n}_\pm\mathcal{D}[a_\pm^\dagger](\rho)+(1+\bar{n}_\pm)\mathcal{D}[a_\pm](\rho)\right)$, and $\mathcal{L}_m(\rho)=\Gamma_m\left(\bar{n}_m\mathcal{D}[b^\dagger](\rho)+(1+\bar{n}_m)\mathcal{D}[b](\rho)\right)$, and where $\bar{n}_\pm=n(T_\pm)$ and $\bar{n}_m=n(T_m)$. The Heisenberg equation of motion for a generic operator O can be written as

$$\begin{aligned}\langle\dot{O}\rangle\ &=\ -i\langle[O,H]\rangle\\ &+\tfrac{\kappa_+}{2}\bar{n}_+\left(\langle[[a_+,O],a_+^\dagger]\rangle+\langle[[a_+^\dagger,O],a_+]\rangle\right)+\tfrac{\kappa_+}{2}\left(\langle[a_+^\dagger,O]a_+\rangle+\langle a_+^\dagger[O,a_+]\rangle\right)\\ &+\tfrac{\kappa_-}{2}\bar{n}_-\left(\langle[[a_-,O],a_-^\dagger]\rangle+\langle[[a_-^\dagger,O],a_-]\rangle\right)+\tfrac{\kappa_-}{2}\left(\langle[a_-^\dagger,O]a_-\rangle+\langle a_-^\dagger[O,a_-]\rangle\right)\\ &+\tfrac{\Gamma_m}{2}\bar{n}_m\left(\langle[[b,O],b^\dagger]\rangle+\langle[[b^\dagger,O],b]\rangle\right)+\tfrac{\Gamma_m}{2}\left(\langle[b^\dagger,O]b\rangle+\langle b^\dagger[O,b]\rangle\right)\ \ .\end{aligned} \tag{57}$$

In the steady state

$$\begin{aligned}\langle a_\pm^\dagger a_\pm\rangle\ &=\ \bar{n}_\pm\\ \langle(a_\pm^\dagger a_\pm)^2\rangle\ &=\ \bar{n}_\pm+2\bar{n}_\pm^2\\ \langle a_+^\dagger a_+a_-^\dagger a_-\rangle\ &=\ \bar{n}_+\bar{n}_-\end{aligned}\qquad\begin{aligned}\langle X\rangle\ &=\ -4\sqrt{2}\alpha\bar{\eta}_m\frac{Q_m}{1+4Q_m^2}\\ \langle\tilde{X}\rangle\ &=\ -2\sqrt{2}\alpha\bar{\eta}_m\frac{1}{1+4Q_m^2}\end{aligned}\ \ , \tag{58}$$

where

$$\begin{aligned}Q_m\ &=\ \frac{\omega_m}{\Gamma_m}\\ \bar{\eta}_m\ &=\ \frac{g_0}{\Gamma_m}=\eta_mQ_m\ \ ,\end{aligned} \tag{59}$$

and

$$\alpha=\langle\hat{\alpha}\rangle=\alpha_+\bar{n}_++\alpha_-\bar{n}_-+\xi\ \ . \tag{60}$$

The cavity zero-point energy contributions neglected in Eq. (58), would lead to an additional temperature-independent term in the previous expression which can be obtained by the replacement $\alpha \mapsto \alpha + 1/2$. Similarly, we can calculate the correlations between the light-matter system and the mechanical mode as

$$\begin{aligned} \langle a_\pm^\dagger a_\pm X \rangle &= \langle X \rangle \bar{n}_\pm - p_\pm \\ \langle a_\pm^\dagger a_\pm \tilde{X} \rangle &= \bar{n}_\pm \langle \tilde{X} \rangle - s_\pm \ , \end{aligned} \tag{61}$$

where

$$\begin{aligned} p_\pm &= 4\sqrt{2} \frac{Q_m \bar{\eta}_m \alpha_\pm \bar{n}_\pm (1+\bar{n}_\pm)}{4Q_m^2 + \beta_\pm{}^2} \\ \beta_\pm &= \frac{\Gamma_m + 2\kappa_\pm}{\Gamma_m} \\ s_\pm &= 2\sqrt{2} \frac{\beta_\pm \bar{\eta}_m \alpha_\pm \bar{n}_\pm (1+\bar{n}_\pm)}{4Q_m^2 + \beta_\pm{}^2} \ . \end{aligned} \tag{62}$$

The mechanical correlations are readily found to be

$$\begin{cases} \langle X\tilde{X} + \tilde{X}X \rangle = \dfrac{2\sqrt{2}}{1+4Q_m^2}(-2\alpha\langle X \rangle + p + 2Q_m s) \\ \langle X^2 \rangle = \bar{n}_m + \frac{1}{2} + \langle X \rangle^2 + 2\sqrt{2}\dfrac{\bar{\eta}_m Q_m}{1+4Q_m^2}(p + 2Q_m s) \\ \langle \tilde{X}^2 \rangle = \bar{n}_m + \frac{1}{2} + \langle \tilde{X} \rangle^2 - 2\sqrt{2}\dfrac{\bar{\eta}_m Q_m}{1+4Q_m^2} p + 2\sqrt{2}\dfrac{\bar{\eta}_m}{1+4Q_m^2}(1+2Q_m^2)s \ , \end{cases} \tag{63}$$

where $p = \alpha_+ p_+ + \alpha_- p_-$ and $s = \alpha_+ s_+ + \alpha_- s_-$, leading to

$$\begin{aligned} \delta\tilde{X}^2 &= \langle \tilde{X}^2 \rangle - \langle \tilde{X} \rangle^2 \\ &\le \tfrac{1}{2} + \bar{n}_m + 2\sqrt{2}\frac{\bar{\eta}_m}{1+4Q_m^2}(1+2Q_m^2)s \\ &\le \tfrac{1}{2} + \bar{n}_m + 8\bar{\eta}_m^2 R \ , \end{aligned} \tag{64}$$

where we used the fact that $\text{argmax}[f(Q_m)] = 0$, where

$$f(Q_m) = \frac{(1+2Q_m^2)}{(1+4Q_m^2)(Q^2+4Q_m^2)} \ , \tag{65}$$

and defined

$$R = \frac{\alpha_+^2}{\beta_+}\bar{n}_+(1+\bar{n}_+) + \frac{\alpha_-^2}{\beta_-}\bar{n}_-(1+\bar{n}_-) \ . \tag{66}$$

Note that the quantity $\langle \tilde{X}^2 \rangle$ is affected from the cavity zero-point energy contributions only through $\langle \tilde{X} \rangle^2$ in Eq. (63). For this reason, the expression for the variance $\delta\tilde{X}^2$ is independent from such contributions.

For completeness, we also report the results for the variance of the other quadrature

$$\begin{aligned} \delta X^2 &= \langle X^2 \rangle - \langle X \rangle^2 \\ &\le \bar{n}_m + \tfrac{1}{2} + 16\bar{\eta}_m^2 \tilde{R} \ , \end{aligned} \tag{67}$$

where we used

$$\text{argmax}(f_X(Q_m)) = \frac{\sqrt{Q}}{2} \ , \tag{68}$$

and defined

$$\tilde{R} = \frac{\alpha_+^2 \bar{n}_+(1+\bar{n}_+)}{4(1+\beta_+)} + \frac{\alpha_-^2 \bar{n}_-(1+\bar{n}_-)}{4(1+\beta_-)} \ . \tag{69}$$

B. Visibility

The modulation of the opto-mechanical coupling $g_0 \mapsto g_0 \cos(\omega_d t)$ effectively corresponds (in a frame rotating at ω_d) to the redefinitions

$$\begin{aligned} g_0 &\mapsto g_0/2 \\ \bar{\eta}_m &\mapsto \bar{\eta}_m/2 \\ \omega_m &\mapsto \delta \ , \end{aligned} \tag{70}$$

where, as a reminder, $\bar{\eta}_m = g_0/\Gamma_m$ and $\delta = \omega_m - \omega_d \ll \omega_m$. In this way, from Eq. (58), the displacement of the quadrature $\tilde{X}$ can be written as

$$|\langle \tilde{X} \rangle| = |\langle \tilde{X} \rangle_{\bar{n}}| + |\langle \tilde{X} \rangle_{\mathrm{GS}}| \ , \tag{71}$$

where

$$\begin{aligned} |\langle \tilde{X} \rangle_{\bar{n}}| &= \frac{\sqrt{2}\bar{\eta}_m}{1+4Q_\delta^2}(\alpha - \xi) \\ |\langle \tilde{X} \rangle_{\mathrm{GS}}| &= \frac{\sqrt{2}\bar{\eta}_m}{1+4Q_\delta^2}\xi \ , \end{aligned} \tag{72}$$

are the thermal (associated with the index $\bar{n}$) and ground state (associated with the index GS) contributions to the total displacement respectively (with $Q_\delta = \delta/\Gamma_m$). Note that these equations differ from Eqs. (58) by a factor 2 due to the re-definitions outlined in Eq. (70). Moreover, the zero-point contribution to the cavity energy calculated in the previous section would effectively add a constant term $|\langle \tilde{X} \rangle|_{zp} = \bar{\eta}_m/\sqrt{2}(1+4Q_\delta^2)$ to the expression in Eq. (71). However, as seen from our previous analysis, such a contribution does not affect the expression for the variances. For this reason, it can simply be subtracted off the average value.

The signal we are interested to resolve is the displacement due to ground-state effects, i.e., $\langle \tilde{X} \rangle_{\mathrm{GS}}$. This makes it natural to define signal-to-noise ratio in the following way

$$F_{\mathrm{GS}} = \frac{|\langle \tilde{X} \rangle_{\mathrm{GS}}|}{\delta \tilde{X}} \ , \tag{73}$$

where, from Eq. (64)

$$\delta \tilde{X}^2 \leq \frac{1}{2} + \bar{n}_m + 2\bar{\eta}_m^2 R \ , \tag{74}$$

where the missing factor 4 in front of $\bar{\eta}_m$ takes into account Eq. (70).

We then want to impose two conditions for the observation of the effect. The first, is the standard quantum limit (SQL) requirement

$$F_{\mathrm{GS}} > 1 \ , \tag{75}$$

for the resolution of the signal. Secondly, we require to be in a regime where ground state effects are predominant with respect to thermal ones, i.e.,

$$|\langle \tilde{X} \rangle_{\mathrm{GS}}| > |\langle \tilde{X} \rangle_{\bar{n}}| \ . \tag{76}$$

Alternatively, dividing both sides by $\delta\tilde{X}$, this condition can be written as $F_{\mathrm{GS}} > F_{\bar{n}}$, where $F_{\bar{n}} = F - F_{\mathrm{GS}}$. In this way, we are equivalently requiring that most of the resolved physical ratio

$$F = \frac{\langle \tilde{X} \rangle}{\delta \tilde{X}} \tag{77}$$

is due to ground state effects. Let us now analyze both of these in more detail. From Eq. (71) we see that the condition for the predominance of ground state effects $F_{\mathrm{GS}} > 1$ takes the simple form $\xi > \alpha - \xi$ or

$$\bar{n} < n_{\mathrm{GS}} = \frac{\eta^2}{4} \ , \tag{78}$$

where we used the definition in Eq. (60), and the expressions for $\alpha_\pm$ and ξ for the spin and bosonic case. Up to second-order in η this expression leads to the result in Eq. (78).

The SQL condition $F_{\rm GS} > 1$ is more complex and involves the mechanical variance. Using the definition in Eq. (73), together with the results in Eqs. (58) and(64) we obtain, through some algebra

$$\bar{\eta}_m > \bar{\eta}_m^{\rm SQL} \quad , \tag{79}$$

where

$$(\bar{\eta}_m^{\rm SQL})^2 = \frac{(1+4Q_\delta^2)^2(1+2\bar{n}_m)}{4(\xi^2-(1+4Q_\delta^2)^2 R)} \quad . \tag{80}$$

The positivity of the left-hand side requires that $R < \frac{\xi^2}{(1+4Q_\delta^2)^2}$, which, to forth-order in η, leads to

$$\bar{n} < n_{\rm SQL} \quad , \tag{81}$$

where

$$n_{\rm SQL} = \frac{1}{8}\beta\frac{\eta^4}{(1+4Q_\delta^2)^2} \quad . \tag{82}$$

We note that the extrapolation of this result at fourth order in η is valid at fourth-order perturbation theory since it depends quadratically on the ground state displacement whose lowest order expansion in η is $O(\eta^2)$), and

$$\beta = \frac{\Gamma_m + 2\kappa}{\Gamma_m} \quad , \tag{83}$$

where $\kappa = \kappa_\pm$ in the case $\eta = 0$. Note that the bound in Eq. (79) explicitly depends on the expressions for $\alpha_\pm$ through the quantity R (defined in Eq. (66)). For this reason its expression as a function of η will depend upon the spin or bosonic case considered. However, the bound in Eq. (81) is, at lowest order in η, common to the two cases.

We can then collect these two conditions to find that

$$\bar{n} < n_{\max} \quad , \tag{84}$$

where

$$n_{\max} = \min\left(\frac{\eta^2}{4}, \frac{1}{8}\beta\frac{\eta^4}{(1+4Q_\delta^2)^2}\right) \quad , \tag{85}$$

is the maximum allowed occupation number for the light-matter system in order to observe the effect. More precisely, we can say that $n_{\max}$ is the maximum occupation number such that a value of g_0 exists for which the effect can be observed. Such a value is given by Eq. (79), which, for $Q_\delta \to 0$ and $\bar{n} = \bar{n}_m = 0$ gives

$$\bar{\eta}_m > \frac{2}{\eta^2} \quad , \tag{86}$$

which sets the best-conditions limit for the observation of the effect.

We summarize the logic and findings of this chapter in the following table.

Requirement	**Condition**	**Physical Contraints**
Standard Quantum Limit	$F_{\rm GS} > 1$	$\bar{n} < n_{\rm SQL}$ $\bar{\eta}_m > \eta_m^{\rm SQL}$
Ground State Effects Physics	$\lvert\langle\tilde{X}\rangle_{\rm GS}\rvert > \lvert\langle\tilde{X}\rangle_{\bar{n}}\rvert$	$\bar{n} < n_{\rm GS}$

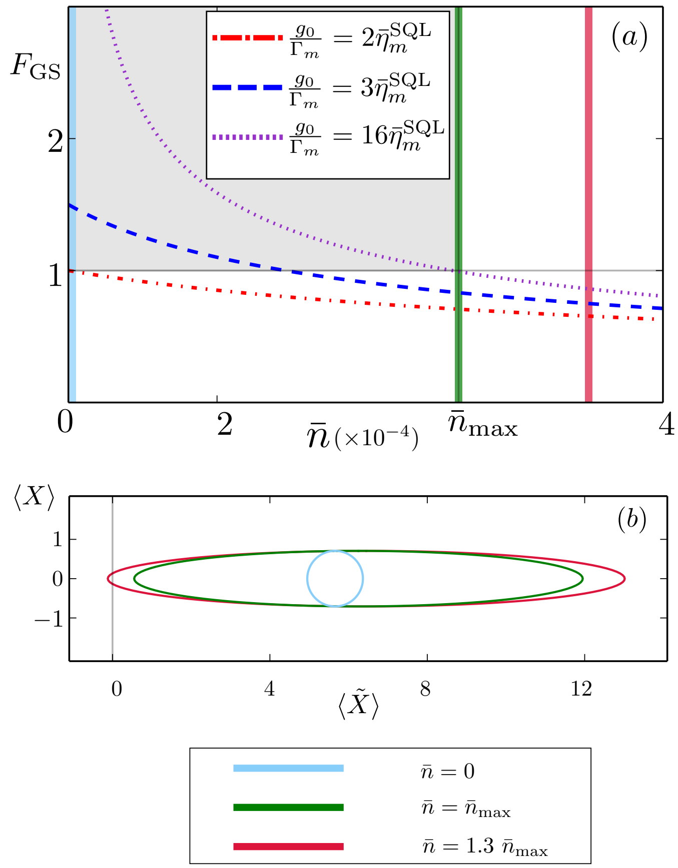

FIG. 1. (a) Ground-state displacement visibility F_{GS} as a function of the number of thermal light-matter excitations $\bar{n}$. This plot follows (with same parameters) the inset of Fig. 1 in the main text and it is reported here to give context to the diagram in (b) where we represent the state of the system with $g_0/\Gamma_m = 16\bar{\eta}_m^{\rm SQL}$ [violet curve in (a)] at different temperatures. At the highlighted values of $\bar{n}$ in (a), in (b) we plot (following a color code) the phasor diagram for the state of the system, i.e. a graphical representation for its quadrature displacement [for $X = (b + b^\dagger)/\sqrt{2}$ and $\tilde{X} = i(b^\dagger - b)/\sqrt{2}$] and standard deviation. This plot is for $g_0/\Gamma_m = 16\bar{\eta}_0^{\rm SQL}$, i.e., it correspondes to the violet curve in (a). For $\bar{n} = 0$ [light-blue line in (a)] the displacement of the oscillator (position of the center of the ellipse) can be clearly resolved with respect to its standard deviation (half the ellipses axis). As $\bar{n}$ is increased [green and red lines in (a)], thermal noise causes the standard deviation to increase (axes of the green and red ellipses). For example, for $\bar{n} > \bar{n}_{\rm max}$ the standard deviation becomes bigger than the actual displacement overtaking the minimal requirement for the observation of the effect set in Eq. (84).

For bookkeeping, the other quadrature gives the following result

$$\begin{aligned} F_X^2 &= \frac{\langle X\rangle^2}{\delta X^2} \\ &\geq \frac{8\alpha^2\bar{\eta}_m^2 Q_\delta^2}{(1+4Q_\delta^2)^2(\frac{1}{2}+\bar{n}_m+4\bar{\eta}_m^2\tilde{R})} \ , \end{aligned} \tag{87}$$

which, with respect to $F_{\tilde{X}}$, is suppressed by a factor Q_δ, which tends towards zero in the amplification approach considered in this article.

Finally, we note that, in the limit for $n_\pm = n \to \infty$, and for $\delta = 0$ (i.e., driving of the opto-mechanical coupling in resonance to the mechanical frequency) we obtain

$$F \to 2\left(\frac{1}{\beta_+} + \frac{1}{\beta_-}\right)^{-\frac{1}{2}} \ . \tag{88}$$

In the same limit, in the absence of matter, we find

$$F_{\eta=0} \to \sqrt{\beta} \ . \tag{89}$$

where $\beta = \Gamma_m/(\Gamma_m + 2\kappa_1)$.

To better exemplify these results, we refer to the phasor diagram in Fig.1b. For clarity, the same Figure also reports the inset of Fig.1 in the main text. At the occupation numbers corresponding to the coloured vertical lines in Fig. 1a, we graphically represent the state of the mechanical oscillator in Fig. 1b. The center of the ellipses represent the quadrature displacements while the length of the ellipses' half-axis represent the corresponding standard deviation.

IV. EXPERIMENTAL FEASIBILITY IN ELECTRO-MECHANICAL SYSTEMS

In this section, we present the details for the experimental feasibility of the system presented in this article. We consider electro-mechanical systems, in particular referring to the work by Teufel et al. [15].

The system built in [15] can be modelled as an LC-circuit (See Fig. 1a) in which the capacitance is modulated by the mechanical motion of a micro-membrane. In the following, we will denote by x the membrane displacement which modulates the circuit capacitance C_x, and by L_0 the circuit inductance. As a consequence, the circuit frequency is also modulated by the mechanical motion as

$$\omega_x \;=\; (L_0 C_x)^{-1/2} = \omega_0 - g_0 x \;\;, \tag{90}$$

where we expanded at first order in x/d, where d is the distance between the plates in the capacitor. The opto-mechanical coupling is defined as

$$g_0 = -\frac{d\omega_x}{dx}_{|x=0} = \frac{\omega_0}{2d} \;\;. \tag{91}$$

We now want to show how to modify this effective model in order to account for a modulation of the opto-mechanical coupling g introduced in the main article. To achieve this we will extend the work by Liao et al. [10].
Let us consider the circuit sketched in Fig. 1b. There, we added a SQUID (capacitor) in series (parallel) to the original L_0 (C_x).
The kinematic inductance L_t of the SQUID can be modulated in time by threading it with an external time-dependent magnetic flux ϕ_t as $L_t = L_J/(2\cos\frac{\Phi_t}{\Phi_0})$, in terms of the reduced flux quantum $\Phi_0 = \hbar/2e$, where e is the charge of the electron, and where L_J is the kinematic inductance of the Josephson junctions composing the SQUID, and where we neglected the self inductance of the SQUID-loop. In the following, we will further neglect additional higher-order non linearities [16].
We assume the additional capacitor (with capacitance C_t) to be electrically tunable [17, 18] (some versions of which are already commercially available [19]).

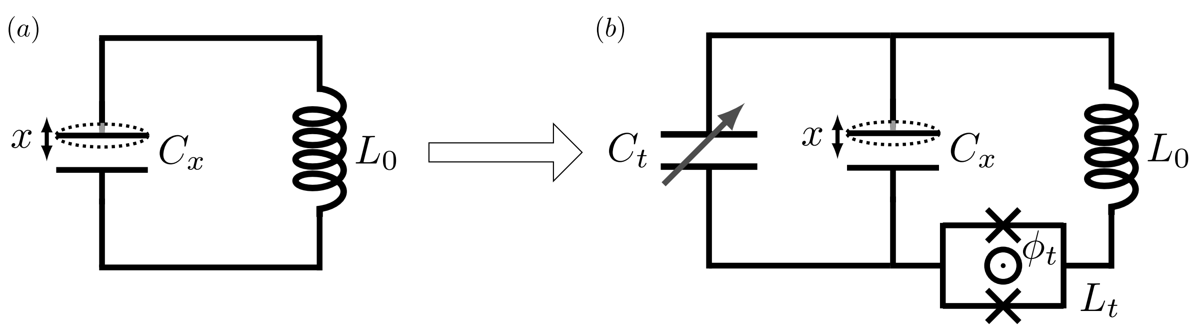

FIG. 2. (a) Method for the opto-mechanical system considered in [15]. A mechanical oscillator modulates the distance between the plates of a capacitor in a LC circuit, inducing an opto-mechanical coupling. (b) By adding an additional tunable inductor (in the form of a SQUID thread by a time-dependent magnetic flux) and a tunable capacitor the opto-mechanical coupling can be further modulated. Such a modulation can be used to amplify weak mechanical signals as those due to virtual radiation pressure when the system is coupled to an atom (see Fig. 1).

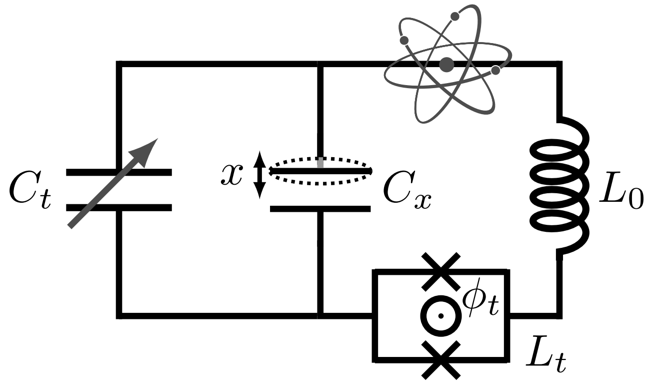

FIG. 3. Method to probe virtual photons in a light-matter ground state in the ultra-strong coupling regime. The virtual photons dressing the ground state displace the oscillator by radiation pressure. An additional SQUID (thread by a time-dependent magnetic flux) and an additional tunable capacitor modulate the opto-mechanical coupling strength, allowing to amplify the mechanical signal.

The main idea is to use these extra-degrees of freedom in order to obtain a time-dependent opto-mechanical coupling while keeping the frequency of the oscillator time-independent. The frequency of the circuit in Fig. 3 is given by

$$\omega_x \;\mapsto\; \left[(L_0+L_t)(C_x+C_t)\right]^{-1/2} = \omega_t - g_t x \quad , \tag{92}$$

where

$$\omega_t \;=\; \frac{\omega_0}{(1+L_t/L_0)(1+C_t/C_0)} \quad , \qquad\qquad g_t \;=\; \frac{\omega_0}{(1+L_t/L_0)(1+C_t/C_0)}\frac{C_0}{2d(C_0+C_t)} \quad . \tag{93}$$

If we now suppose that $C_t = C_0 + \zeta C_0 \cos\omega_m t$ with $0 < \zeta < 1$, and that

$$\frac{L_t}{L_0} = -\frac{1+\zeta\cos\omega_m t}{2+\zeta\cos\omega_m t} \quad , \tag{94}$$

the previous expressions simplify as

$$\omega_x \;=\; \omega_0 + g_t x \quad , \tag{95}$$

with

$$g_t/g_0 = -1 + \frac{\zeta}{4}\cos\omega_m t - \frac{(\zeta\cos\omega_m t)^2}{8} + \frac{(\zeta\cos\omega_m t)^3}{16} \quad , \tag{96}$$

where we neglected higher order terms $O(\zeta^4)$.

To make contact with our previous results, we now need to consider the replacement $\omega(x) \mapsto \omega_x$ in Eq. (1), considering $\omega \equiv \omega_0$. By doing this, the same rotating wave approximation (valid because $g_0/\omega_m \ll 1$) considered after Eq. (18) will give an effective opto-mechanical coupling

$$g_t \to g_t^{\mathrm{eff}} = g_0\left(\frac{\zeta}{4}+\frac{\zeta^3}{32}\right)\cos\omega_m t \quad . \tag{97}$$

As shown by the protocol presented in this article, by coupling the resonator to a superconducting atom (see Fig. 3), this modulation of the opto-mechanical coupling allows to probe the light-matter ground state in the ultra-strong coupling regime.

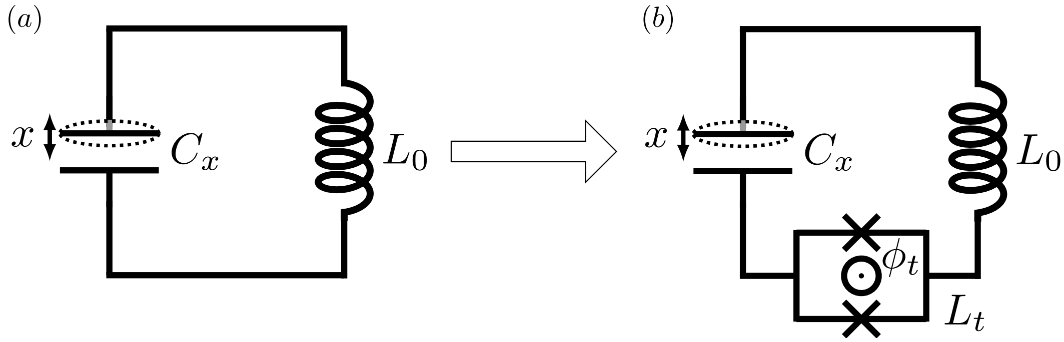

FIG. 4. Simplification of the scheme represented in Fig. 1. In (b), the modulation of the kinetic inductance in the SQUID causes an effective modulation of both the frequency and the opto-mechanical coupling for the circuit described in (a). However, since the frequency modulation is slow with respect to the light-matter resonant frequency, this leads to the same low-temperature results as in the presence of the tunable capacitor.

A. Alternative method

A different (low-temperature) analysis can lead to amplification of the ground-state signal, even in the absence of the tunable capacitor (see Fig. 4). In this case, the frequency of the circuit in Fig. 4 is given by

$$\omega_x \;\mapsto\; [(L_0+L_t)C_x]^{-1/2} = \omega_t - g_t x \quad , \tag{98}$$

where

$$\omega_t \;=\; \omega_0(1+L_t/L_0)^{-1/2} \quad , \qquad\qquad g_t \;=\; g_0(1+L_t/L_0)^{-1/2} \quad . \tag{99}$$

In the following we will choose $L_t/L_0 = \zeta\cos(\omega_m t)$, with $\zeta < 1$. From the expression above we can note that, in this approach, not only we modulate the opto-mechanical coupling, but also the cavity frequency. However, this is not necessarily detrimental for the amplification of the ground-state signal we are interested in. To see this, let us first focus on the light-matter system described by the Rabi Hamiltonian given in Eq. (4) with $\omega \mapsto \omega_t$.

First of all, we notice that the adiabatic theorem assures that the transitions between eigenstates of the systems (calculated at any given time) caused by the parametric modulation of the frequency are negligible, mainly due to the fact that $\omega_m \ll \omega_0$. More precisely (see [20], chapter 10), errors to the adiabatic evolution can be quantified as $O(|\dot{H}_R(t)_{pq}/\Delta|)$, where $\Delta = \min_t[E_q(t) - E_p(t)]$, where $\dot{H}_R(t)_{pq} = \langle p|\,\dot{H}(t)\,|q\rangle$, with $|q(t)\rangle$ ($E_q(t)$) the eigenstates of H_R in Eq. (4), under the substitution $\omega(x) \mapsto \omega_x$ for a fixed t, and where $H_R(t) \propto \cos\omega_m t$ is the time-dependent part of the quantum Rabi Hamiltonian.
Let us now consider the system to be in the ground state (compatibly with the low-temperature assumptions used throughout this article). The adiabatic approximation holds provided that [20]

$$O(|\dot{H}_R(t)_{pq}/\Delta|) < O(|H(t)|_{pq}) \quad . \tag{100}$$

In the ultra-strong coupling regime, the light-matter system is gapped and $\Delta = O(\omega_0)$, at lowest order in η. Since $H(t) \propto \cos\omega_m t$, we also have $O(|\dot{H(t)}_{pq}/\Delta|) = \omega_m O(|H(t)|_{pq})$, which satisfies the adiabatic hypothesis under the physically justified assumption $\omega_m \ll \omega$. Under these conditions, the light-matter system adiabatically follows the ground state in its dynamics, which, in the presence of the probe, is described by (see Eq. (18))

$$H^{\rm eff} = g_t\frac{\eta_t^2}{4}(b+b^\dagger) + \omega_m b^\dagger b \quad . \tag{101}$$

In the previous expression we took into account that the normalized coupling $\eta = \Omega/\omega_0$ has now to be re-defined following Eq. (99), and the fact that, upon the modulation of the cavity frequency, the light-matter system is not at resonance all the time i.e., $\eta \mapsto \eta_t$, where $\eta_t/2 = \Omega/(\omega_t+\omega_0)$. From Eqs. (101) and (99) we finally find that, when the light-matter system is in the ground state, the system is described by the following effective Hamiltonian

$$H^{\rm eff} = \frac{g_0}{\left(1+\sqrt{1+\zeta\cos\omega_m t}\right)}\eta^2(b+b^\dagger) + \omega_m b^\dagger b \quad . \tag{102}$$

Following the same reasoning that lead us to Eq. (97), after a rotating-wave approximation the effective opto-mechanical coupling becomes

$$g_t \to g^{\text{eff}} = -g_0 \left(\frac{\zeta}{8} - \frac{\zeta^3}{256} \right) \cos \omega_m t \ \ . \tag{103}$$

In conclusion, the analysis given above shows that modulating the opto-mechanical coupling in an electro-mechanical system is experimentally feasible with state-of-the-art technology.

[1] M. Aspelmeyer, T. J. Kippenberg, and F. Marquardt, "Cavity optomechanics," Reviews of Modern Physics **86**, 1391–1452 (2014), arXiv:1303.0733.

[2] W. P. Bowen and G. J. Milburn, *Quantum Optomechanics* (Taylor & Francis, Boca Raton, Florida, 2015).

[3] Y. Chang, H. Ian, and C.P. Sun, "Triple coupling and parameter resonance in quantum optomechanics with a single atom," Journal of Physics B **42**, 215502 (2009), arXiv:0810.4206.

[4] H.-P Breuer and F. Petruccione, *The theory of open quantum systems* (Oxford University Press, 2002).

[5] F. Beaudoin, J. M. Gambetta, and A. Blais, "Dissipation and ultrastrong coupling in circuit QED," Physical Review A **84**, 043832 (2011), arXiv:1107.3990.

[6] M. Leskes, P. K. Madhu, and S. Vega, "Floquet theory in solid-state nuclear magnetic resonance," Progress in Nuclear Magnetic Resonance Spectroscopy **57**, 345 – 380 (2010).

[7] I. Scholz, B. H. Meier, and M. Ernst, "Operator-based triple-mode Floquet theory in solid-state NMR," The Journal of Chemical Physics **127**, 204504 (2007).

[8] M. Bukov, L. D'Alessio, and A. Polkovnikov, "Universal high-frequency behavior of periodically driven systems: from dynamical stabilization to Floquet engineering," Advances in Physics **64**, 139–226 (2015).

[9] A. Eckardt and E. Anisimovas, "High-frequency approximation for periodically driven quantum systems from a Floquet-space perspective," New Journal of Physics **17**, 093039 (2015), arXiv:1502.06477.

[10] J.-Q. Liao, K. Jacob, F. Nori, and R. W. Simmonds, "Modulated electromechanics: large enhancements of nonlinearities," New Journal of Physics **16**, 072001 (2014), arXiv:1304.4608.

[11] B. Royer, A. L. Grimsmo, N. Didier, and A. Blais, "Fast and high-fidelity entangling gate through parametrically modulated longitudinal coupling," arXiv:1603.04424 (2016).

[12] A. A. Zhukov, D. S. Shapiro, W. V. Pogosov, and Yu. E. Lozovik, "Dynamical Lamb effect versus dissipation in superconducting quantum circuits," Phys. Rev. A **93**, 063845 (2016), arXiv:1603.02040.

[13] D. S. Shapiro, A. A. Zhukov, W. V. Pogosov, and Yu. E. Lozovik, "Dynamical Lamb effect in a tunable superconducting qubit-cavity system," Phys. Rev. A **91**, 063814 (2015), arXiv:1503.01666.

[14] H. J Carmichael, *Statistical Methods in Quantum Optics 1: Master Equations and Fokker-Planck Equations* (Springer-Verlag Berlin Heidelberg, 1999).

[15] J. D. Teufel, T. Donner, D. Li, J. W. Harlow, M. S. Allman, K. Cicak, A. J. Sirois, J. D. Whittaker, K. W. Lehnert, and R. W. Simmonds, "Sideband cooling of micromechanical motion to the quantum ground state." Nature **475**, 359–63 (2011), arXiv:1103.2144.

[16] A. Palacios-Laloy, F. Nguyen, F. Mallet, P. Bertet, D. Vion, and D. Esteve, "Tunable resonators for quantum circuits," Journal of Low Temperature Physics **151**, 1034–1042 (2008).

[17] T. Vaha-Heikkila, J. Varis, J. Tuovinen, and G. M. Rebeiz, "A reconfigurable $6-20$ GHz RF MEMS impedance tuner," in *2004 IEEE MTT-S International Microwave Symposium Digest (IEEE Cat. No.04CH37535)*, Vol. 2 (2004) pp. 729–732 Vol.2.

[18] R. L. Borwick, P. A. Stupar, J. DeNatale, R. Anderson, C. Tsai, K. Garrett, and R. Erlandson, "A high Q, large tuning range MEMS capacitor for RF filter systems," Sensors and Actuators A: Physical **103**, 33 – 41 (2003).

[19] https://www.johansontechnology.com/lasertrim-rf-tuning (2017).

[20] D. J. Griffiths, *Introduction to Quantum Mechanics* (Prentice Hall Inc., 1995).